



# Synthesis and luminescent properties of Zn complex based on 8-hydroxyquinoline group containing 3,5-bis(trifluoromethyl) benzene unit with unique crystal structure

Yan-Ping Huo<sup>a,b</sup>, Shi-Zheng Zhu<sup>b,\*</sup>, Sheng Hu<sup>a</sup>

<sup>a</sup> Faculty of Chemical Engineering and Light Industry, Guangdong University of Technology, Guangzhou 510006, China

<sup>b</sup> Key Laboratory of Organofluorine Chemistry, Shanghai Institute of Organic Chemistry, Chinese Academy of Sciences, Shanghai 200032, China

## ARTICLE INFO

### Article history:

Received 20 July 2010

Received in revised form 8 September 2010

Accepted 10 September 2010

Available online 17 September 2010

### Keywords:

8-Hydroxyquinoline

Metal complex

Crystal structure

Luminescence properties

## ABSTRACT

The use of a novel 2-substituted-8-hydroxyquinoline ligand (*E*)-2-{2-[3,5-bis(trifluoromethyl)phenyl]ethenyl}-8-hydroxyquinoline (**4**, BFHQ) characterized by EIMS, <sup>1</sup>H NMR spectroscopy, elemental analysis, and FTIR spectroscopy enabled the isolation of a trimeric Zn(II) complex with the formula Zn<sub>3</sub>(BFHQ)<sub>6</sub> (**5**, Scheme 1). X-ray structural analysis shows that **5** exhibits a trinuclear core, which is bridged by four 8-hydroxyquinoline rings. The trinuclear core is surrounded by three pairs of BFHQ ligands with offset π–π stacking, showing propeller-like molecular structure. The aggregation behavior of Zn(AcO)<sub>2</sub> and the ligand **4** in solution was investigated by UV–vis. The luminescence properties of compound **5** were investigated by UV–vis and fluorescence spectra at room temperature. The experimental results show that the complex **5** emits yellow luminescence at 553 nm (λ<sub>em, max</sub>) in DMSO solution and at 610 nm (λ<sub>em, max</sub>) in solid state. The thermogravimetric analysis was carried out to examine the thermal stability.

© 2010 Elsevier Ltd. All rights reserved.

## 1. Introduction

Since Tang and VanSlyke developed multi-layered organic light-emitting diodes (OLEDs) using tris-(8-hydroxyquinoline)aluminum (AlQ<sub>3</sub>) as the emission and electron transport material,<sup>1</sup> much effort has been made to the development of highly efficient OLEDs,<sup>2–4</sup> especially the white OLEDs.<sup>5–8</sup> To obtain white emission, various strategies have been developed. For small-molecule OLEDs, the general approach is to fabricate multiplayer devices by consecutive evaporation involving three primary colors (blue, green, and red) or two special colors (blue and yellow). However, multiplayer construction of devices will increase the cost of fabrication processes. In order to reduce the cost and obtain white OLEDs with minimal process of fabrication, it would be necessary to discover multi-function and highly efficient yellow-light emitting materials.

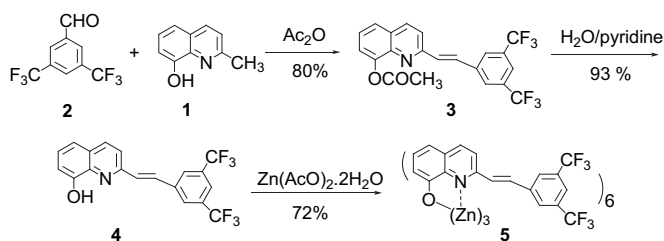
8-Hydroxyquinoline aluminum (AlQ<sub>3</sub>) has been identified as an excellent green-light emitting and electronic transporting material.<sup>1</sup> In order to retain the excellent photoelectron properties of 8-hydroxyquinoline itself and achieve yellow-light emission, a feasible approach is to modify the 2-, 5- or 7-position of the 8-hydroxyquinoline rings with different functional groups.<sup>9–14</sup> For example, Cui<sup>10</sup> reported 2-substituted-8-hydroxyquinoline molecules with

large conjugated groups and tuned their luminescence to yellow-light (λ<sub>em</sub>=610 nm). On the other hand, the fluorinated organic semiconductors have been reported to possess a high electron mobility, excellent air-stability, low sublimation temperature, and perhaps a broadened energy gap, because of the strong electron-withdrawing properties of the fluorine atom.<sup>15,16</sup> It is supposed that highly efficient yellow-light emitting materials could be realized from fluorinated MQ<sub>n</sub> derivatives. However, related reports on fluorinated MQ<sub>n</sub> derivatives are rare so far.<sup>17,18</sup> In addition, research suggests that the electron-transporting mobility of zinc complexes with 8-hydroxyquinoline goes beyond that of aluminum complexes, which is the most widely used electron-transporting material in OLEDs. Thus zinc complexes may be potential candidates to enhance the electron-transporting properties for OLEDs.<sup>24,25</sup> Inspired by these results, we designed and synthesized the novel ligand: (*E*)-2-{2-[3,5-bis(trifluoromethyl)phenyl]ethenyl}-8-hydroxyquinoline (**4**) and the corresponding Zn complex: Zn<sub>3</sub>(BFHQ)<sub>6</sub>.<sup>13</sup> It is expected that a combination of 3,5-bis(trifluoromethyl) benzene unit and 8-hydroxyquinoline could not only retain the excellent photoelectron properties of 8-hydroxyquinoline itself but also achieve yellow-light emission.

We report herein the first synthesis of light-emitting molecule Zn<sub>3</sub>(BFHQ)<sub>6</sub>, which contains the 3,5-bis(trifluoromethyl) benzene moiety and 8-hydroxyquinoline derivative. The synthetic strategies for light-emitting molecule **5** is outlined in Scheme 1. We also investigated its thermal stability, fluorescence property, and crystal

\* Corresponding author. Tel.: +86 21 54925185; fax: +86 21 64166128; e-mail address: zhusz@mail.sioc.ac.cn (S.-Z. Zhu).

structure, which indicated that **5** emits yellow luminescence at 553 nm ( $\lambda_{em, max}$ ) in DMSO solution and at 610 nm ( $\lambda_{em, max}$ ) in solid state, and has a highly symmetrical structure belonging to space group of  $C2/c$ .



Scheme 1.

## 2. Results and discussion

### 2.1. $^1\text{H}$ NMR and FTIR spectra

The  $^1\text{H}$  NMR spectra of **4** and **5** in  $(\text{CD}_3)_2\text{SO}$  solvent are shown in Fig. 1. In the  $^1\text{H}$  NMR spectrum of **4** the proton signals at 9.58, 8.35–8.43, 8.06, 7.87, 7.76, 7.38–7.47, 7.13 can be easily assigned to each the corresponding hydrogen, respectively, which indicate the presence of the hydroxyquinoline and vinylene. The proton signal at 9.58 ppm corresponds to H–O proton of the quinoline. One doublet at 7.87 with a coupling constant=15.9 Hz, indicates the presence of trans configuration in the vinylene units. In the  $^1\text{H}$  NMR spectrum of **5** the proton signals at 8.85, 8.49, 8.39, 8.19, 8.10, 8.04, 7.04, 6.93 can also be easily assigned to each the corresponding hydrogen, respectively. Compared to that of the ligand **4**, the proton signal at 9.58 ppm corresponding to H–O proton of the quinoline is not observed in the  $^1\text{H}$  NMR spectrum of **5**. Two doublets at 8.85, 8.04 with a coupling constant=16.5 Hz, indicate the presence of trans configuration in the vinylene units. Overall, the resonances in the pyridyl ring of the complex **5** shifted downfield with respect to that of the free ligand, and the resonances in the phenoxide ring of the complex **5** shifted upfield with respect to that of the free ligand (Fig. 1). These results indicate the occurrence of the coordination between the ligand **4** and  $\text{Zn}(\text{OAc})_2$ .

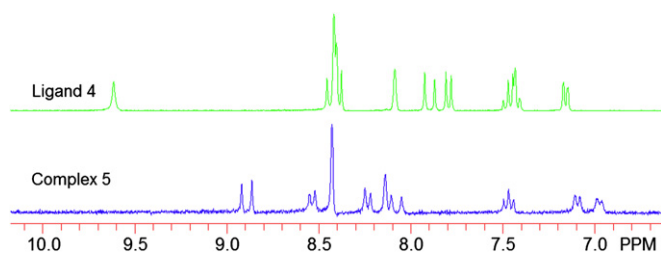


Fig. 1.  $^1\text{H}$  NMR spectra of **4** and **5**.

The absorption peak of O–H is observed at  $3365\text{ cm}^{-1}$ , the absorption peak at  $1693\text{ cm}^{-1}$  is assigned to C=C bond stretching frequency, respectively, in the IR spectrum of the ligand **4**. A sharp peak at  $743\text{ cm}^{-1}$  can be assigned to the out of-plane bending mode of the transvinylene groups, suggesting that the generated double bond is mainly in the trans-configuration. The IR spectrum of the complex **5** has similar absorption bands but a little shift, compared to that of the ligand **4**. The C=C band shifts to  $1638\text{ cm}^{-1}$ . The absorption band at  $3365\text{ cm}^{-1}$  corresponding to O–H stretching frequency is not observed in the IR spectrum of the complex **5**. At the same time, some new sharp bands are observed at  $566\text{--}505\text{ cm}^{-1}$  for **5**, which assigned to the  $\nu(\text{M}–\text{O})$  stretching vibration, and observed at  $496\text{--}442\text{ cm}^{-1}$  for **5**, which assigned to the  $\nu(\text{M}–\text{N})$  stretching vibration.<sup>19,20</sup>

### 2.2. Structure description

X-ray structural analysis shows that **5** has a highly symmetrical structure belonging to space group of  $C2/c$ . The asymmetric unit contains one half of a formula unit, that is, 1.5 unique Zn(II) atoms (Zn1 lies in a general position and Zn2 lies in a special position) and three BFHQ ligands. The structure of **5** is built around a trimeric Zn(II) structure (Fig. 2a). Three pairs of BFHQ ligands with offset face-to-face  $\pi$ – $\pi$  stacking are arranged around the trimeric Zn(II) core in a propeller-like form to generate a supramolecular chiral molecule, in which chirality arises from the chelate Zn(II) centers. Although the trimeric cluster is chiral, two enantiomers are present in the same crystal ( $C2/c$  space group, Fig. 3). The zinc atoms (Zn1 and Zn1A) found on either end of the trimeric unit is pentacoordinate, resulting in a distorted trigonal bipyramidal geometry, and the central zinc atom (Zn2) is hexacoordinate, resulting in a highly distorted octahedral geometry. Four of the BFHQ ligands are involved in bridging through the phenolato oxygens, while the remaining two terminal ligands are bound to Zn(1) atoms only. In detail, the Zn1 atom adopts a trigonal bipyramidal geometry with the equatorial plane occupied by the N2O donors of three ligands around the Zn1 and the apical position by two phenol oxygen atoms. The Zn1–N and Zn1–O bond lengths range from 2.147(4) to 2.228(4) Å and from 1.953(3) to 2.041(3) Å, respectively, the cis-bond angles around the Zn1 atom range from  $79.14(13)^\circ$  to  $124.99(15)^\circ$ , while the trans-bond angle is  $125.05(13)^\circ$ . The coordination environment of the Zn2 ion is a distorted octahedron and the equatorial

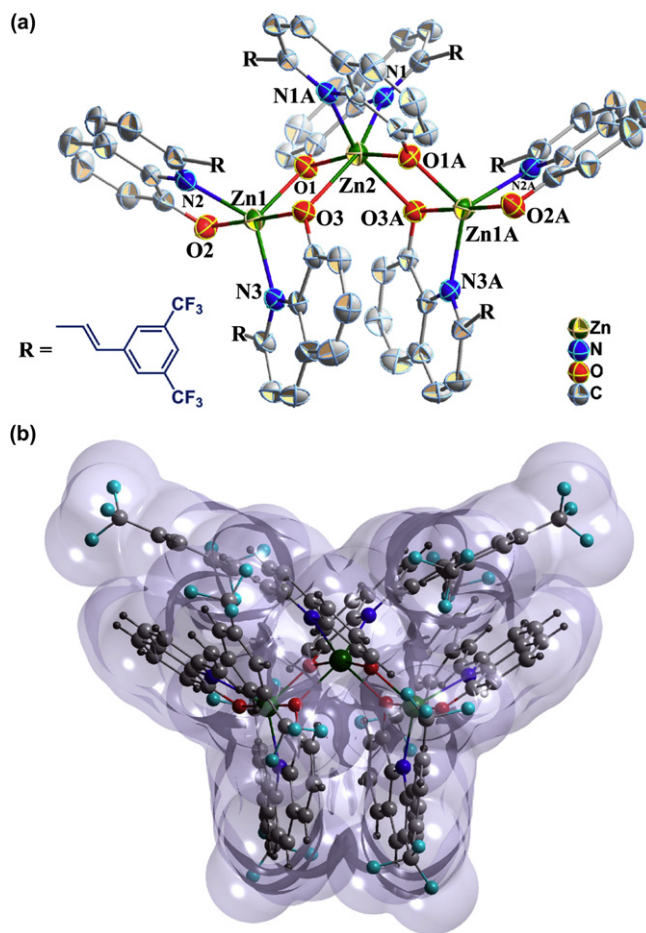


Fig. 2. (a) Perspective views of the coordination geometries of Zn(II) atoms in **5** (some equivalent atoms have been generated to complete the Zn coordination, H atoms omitted for clarity). (b) Space-filling and stick-and-ball representation of the propeller structure of **5**.

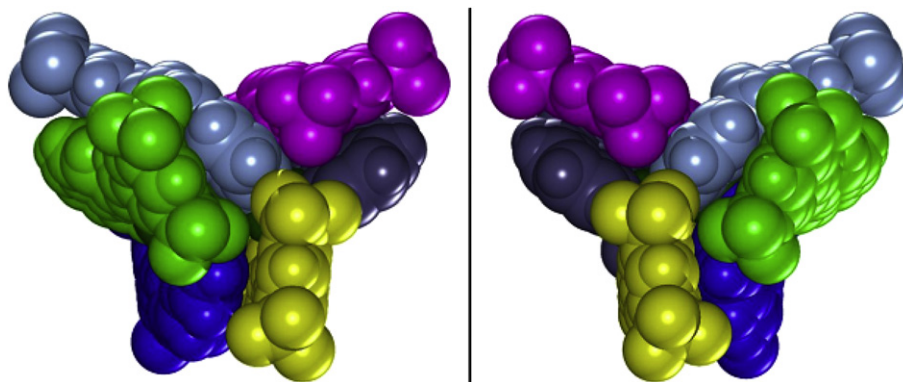


Fig. 3. Space-filling representation of the two enantiomers present in **5**. For clarity each BFHQ ligand is represented in a different color.

plane occupied by the NO<sub>3</sub> donors of three ligands, while the apical position by one phenol oxygen atom and a pyridine atom. The Zn2–N bond lengths are 2.208(4) Å and Zn2–O bond lengths range from 1.992(3) to 2.208(3) Å, respectively, the cis-bond angles around the Zn2 atom range from 75.74(13) to 109.39(14)°, while the trans-bond angles range from 154.82(14)° to 167.79(16)°.

There are significant hydrogen bonds in **5**. Weak nonclassical C–H⋯O intramolecular hydrogen bonds between the phenolato oxygen and the C–H group of quinoline ring or ethenyl (C⋯O=2.995–3.232 Å; C–H⋯O=140.0°–150.0°) as well as intermolecular nonclassical C–H⋯F hydrogen bonds involving the aromatic C–H groups and trifluoromethyls of adjacent 3,5-bis(trifluoromethyl)benzene units of BFHQ ligands (C⋯F=2.704–3.325 Å; C–H⋯F=100°–142°) play a vital role in the consolidation of the solid structure (Fig. 4). Moreover, it is notable that each cluster of **5** involves abundant intramolecular π–π stacking interactions. As shown in Fig. 3, almost all aromatic rings of BFHQ possess significant offset face-to-face π–π stacking interactions with closest interplanar and centroid–centroid separations are in 3.07–3.51 and 3.62–3.62 Å, respectively.

3,5-bis(trifluoromethyl) benzene moiety. The absorption bands of the complex **5** exhibit a red shift comparing to that of ligand **4**, which can be attributed to the increasing conjugated degree of the complex.

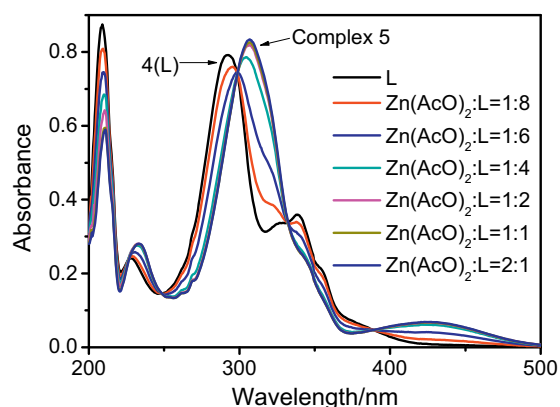


Fig. 5. UV–vis titrations of L (methanol) with Zn(AcO)<sub>2</sub> (H<sub>2</sub>O).

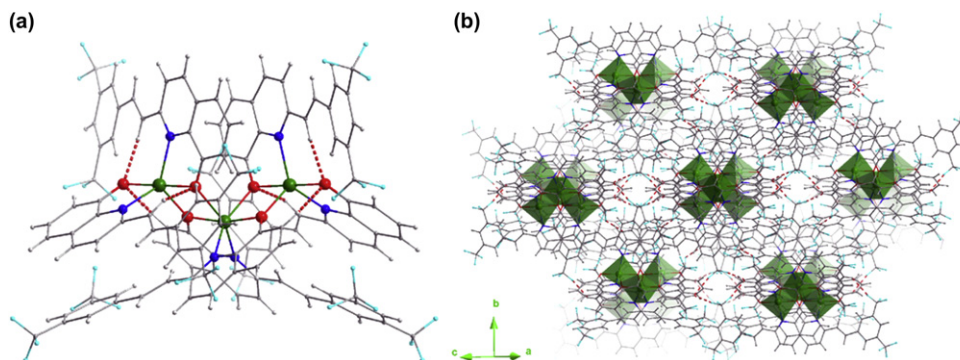


Fig. 4. (a) The trinuclear zinc molecule of **5** and its C–H⋯O intramolecular hydrogen bonding (red dashed lines) are included. (b) The supramolecular 3D structure of **5** mediated by C–H⋯F hydrogen bonding (red dashed lines).

### 2.3. UV–vis absorption titration

The UV–vis absorption spectra of **4** (L) and complex **5** in methanol solution are shown in Fig. 5. The absorption spectrum of **4** contains four bands at 209, 226, 300, and 345 nm, whereas the absorption spectrum of **5** contains four bands at 209, 233, 308, and 430 nm. In the absorption spectrum of the ligand **4** the absorption band at 300 nm originates from intraligand π–π\* transition of quinoline moiety. While, the absorption at around 345 nm is attributed to the charge transfer from the quinoline moiety to the

In order to investigate the interaction mode of ligand **4** (L) with Zn(II) ion in solution, the coordination reaction of L with Zn(II) ion was monitored through a UV–vis spectroscopic titration. After the addition of Zn(II) ion, the absorption band of **4** at 209 nm exhibits hypochromism 35% for **5**, while the absorption bands of **4** at 226 and 300 nm showed significant bathochromism about 7 and 8 nm for those of **5** at 233 and 308 nm. From the absorption spectrum of **4** at 345 nm, in the presence of increasing amounts of Zn(II) ion, the peak was found to become weak and disappear in the end; thus a new band at 430 nm can be observed in the absorption spectrum

of complex **5**. No differences were observed in the absorption spectra after the 1:2 ratio of Zn(II)/L, as shown in Fig. 5, so this experiment clearly showed that the coordination reaches the end point at a 1:2 ratio of Zn(II)/L.

## 2.4. Fluorescence emission spectra

Luminescent properties of compounds **4** and **5** were investigated in DMSO solution and in solid state at room temperature. The fluorescence emission spectra of ligand **4** and the complex **5** are shown in Figs. 6 and 7. The luminescent data of the compounds are summarized in Table 1. The fluorescent spectra of **4** and **5** display maximum emission wavelengths at 473 and 553 nm with excitation wavelengths at 436 and 467 nm in DMSO solution, and maximum emission wavelengths at 487 and 610 nm with excitation wavelengths at 342 and 330 nm in the solid state, respectively. The results indicate that the complex **5** has yellow-light emission in DMSO solution and in the solid state, respectively. The emission of the complex **5** in the solid state predominantly originates from metal-to-ligand charge transfer (MLCT) transition.

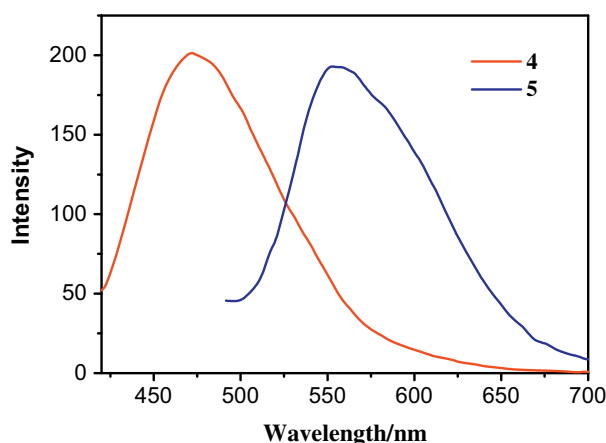


Fig. 6. Emission spectra of the ligand **4** and Zn complex **5** in DMSO.

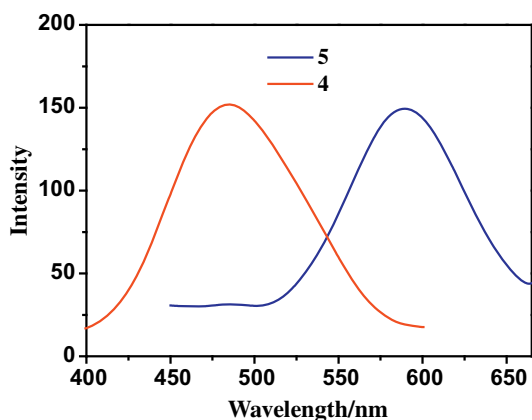


Fig. 7. Emission spectra of the ligand **4** and Zn complex **5** in solid state.

**Table 1**  
Luminescent properties of the ligand **4** and complex **5**

Compounds	Absorption (nm)	Fluorescence spectra (nm)			
		In DMSO ( $10^{-4}$ M)		In solid	
		$\lambda_{em, max}$	$\lambda_{ex, max}$	$\lambda_{em, max}$	$\lambda_{ex, max}$
<b>4</b>	209, 226, 300, 345	473	436	487	342
<b>5</b>	209, 233, 308, 430	553	467	610	330

Compared with the ligand **4**, the corresponding complex **5** exhibits a red shift in DMSO solution and in the solid state, the reason has two-folds: the coordination of metal ions enhances the mobility of the electron transition in backbone due to back-coupling  $\pi$ -bond between the metal and the ligand, and decreases the electron transition energy of intraligand charge transfer. On the other hand, the ligand is coordinated with metal ions to form additional five-membered rings, which increases the  $\pi$ - $\pi^*$  conjugation length and the conformational coplanarity, accordingly reduces the energy gap between the  $\pi$  and  $\pi^*$  molecular orbital of the ligand.<sup>21</sup>

## 2.5. Thermal stability

In the TGA curve of complex **5** (Fig. 8), the thermal degradation temperature  $T_d$  (5% weight loss) is 347 °C, furthermore, the char yield of **5** at 800 °C is 16.5%. From TGA results, the polymeric complex is found to have formed stable five-membered chelate rings,<sup>22</sup> which may be attributed to the fact that the M–N and M–O bonds are highly polarized.<sup>23</sup>

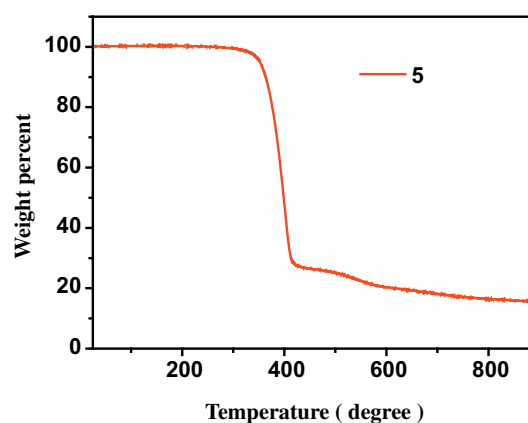


Fig. 8. TGA curve of **5**.

## 3. Conclusion

In summary, a propeller-like trinuclear complex  $Zn_3(BFHQ)_6$  is constructed by self-assembly of Zn(II) ions with a novel 2-substituted-8-hydroxyquinoline ligand. Unlike 8-hydroxyquinoline ligands with a short and rigid spacer that are generally used for the constructions of tris-(8-hydroxyquinoline)aluminum analogs, aromatic stacking interactions and nonclassical C–H $\cdots$ F hydrogen bonds derived from pendant 3,5-bis(trifluoromethyl)benzene group of the BFHQ ligand may play a vital role in the formation of the solid structure and increasing the structural stabilities. Moreover, the aggregation behavior of  $Zn(AcO)_2$  and the BFHQ ligand in solutions was investigated by UV–vis. The luminescence properties of compound (**5**) were investigated by UV–vis and fluorescence spectra at room temperature. The experimental results show that the complex **5** emits yellow luminescence at 553 nm ( $\lambda_{em, max}$ ) in DMSO solution and at 610 nm ( $\lambda_{em, max}$ ) in solid state.

## 4. Experimental section

### 4.1. Chemicals and instruments

All of the chemicals and reagents were purified before use. The FTIR spectra were obtained on a Nicolet AV-360 spectrometer (KBr pellet). NMR spectra were recorded on a Bruker NMR AM-300 spectrometer at room temperature in DMSO- $d_6$  or  $CDCl_3$  using TMS

as the internal reference. Lower resolution mass spectra were obtained on an Applied Biosystems Mariner time-of-flight mass spectrometer using an electrospray ionization technique (ESI). The elemental analysis is achieved on a PerkinElmer 2400 micro-analyser. Thermogravimetric analysis (TGA) was conducted under nitrogen atmosphere at a heating rate 20 K min<sup>-1</sup> with a Shimadzu TGA-7. Ultraviolet–visible (UV–vis) spectra were measured with Shimadzu UV-2501 spectrophotometer. The fluorescence spectra were conducted on a PerkinElmer LS55 luminescence spectrometer with a xenon lamp as the light source.

## 4.2. Synthesis

**4.2.1. Synthesis of (E)-2-[2-[3,5-bis(trifluoromethyl)phenyl]ethenyl]-8-acetoxyquinoline (3).** To a solution of 8-hydroxyquinoline (1) (0.68 g, 4.25 mmol) in acetic anhydride (5 mL) was added 3,5-bis(trifluoromethyl)benzaldehyde (1.0 g, 4.13 mmol). The mixture was heated under reflux for 10 h. After cooled, it was subsequently poured into ice water (50 mL) and stirred overnight. The yellow solid obtained was filtered and washed with water. The solid residue was recrystallized from CH<sub>2</sub>Cl<sub>2</sub> to afford **3** (1.4 g, 80%): mp 159–161 °C; <sup>1</sup>H NMR (CDCl<sub>3</sub>, 300 MHz) δ 8.20 (d, J=8.4 Hz, 1H), 8.02 (s, 2H), 7.82 (s, 1H), 7.72 (d, J=16.2 Hz, 1H), 7.72 (dd, J=9.6 Hz, J=1.2 Hz, 1H), 7.67 (d, J=8.7 Hz, 1H), 7.53 (d, J=16.2 Hz, 1H), 7.44–7.52 (m, 2H), 2.59 (s, 3H); <sup>19</sup>F NMR (CDCl<sub>3</sub>, 282 MHz) δ -63.76 (6F, s); IR (KBr, cm<sup>-1</sup>): 3056, 1717, 1593, 1502, 1433, 1285, 1126, 977, 868, 756, 700; ESI-MS *m/z*: 426.5([M+H]<sup>+</sup>); elemental analysis: found C: 59.24, H: 3.20, N: 3.10 calculated for (C<sub>21</sub>H<sub>13</sub>F<sub>6</sub>NO<sub>2</sub>) C: 59.30, H: 3.08, N: 3.29 (%).

**4.2.2. Synthesis of (E)-2-[2-[3,5-bis(trifluoromethyl)phenyl]ethenyl]-8-hydroxyquinoline (BFHQ) (4).** A solution of acetoxyquinoline **3** (0.85 g, 2.0 mmol) in pyridine (10 mL) was heated under reflux, water (5 mL) was then added, and the reaction mixture refluxed for 3 h. After the mixture cooled, water (20 mL) was added to the mixture. The yellow solid obtained was filtered and washed with water and dried in vacuo to give compound of **4** (0.71 g, 93%): mp 186–188 °C; <sup>1</sup>H NMR (d<sub>6</sub>-DMSO, 300 MHz) δ 7.13 (dd, J=7.0 Hz, J=1.7 Hz, 1H), 7.38–7.47 (m, 2H), 7.76 (d, J=8.1 Hz, 1H), 7.87 (d, J=15.9 Hz, 1H), 8.06 (s, 1H), 8.35–8.43 (m, 4H), 9.58 (s, 1H); <sup>19</sup>F NMR (CDCl<sub>3</sub>, 282 MHz) δ -61.38 (s, 6F); IR (KBr, cm<sup>-1</sup>): 3365, 3052, 1693, 1567, 1517, 1468, 1381, 1276, 1162, 1127, 965, 890, 843, 743, 682; ESI-MS *m/z*: 383.9 ([M+H]<sup>+</sup>); elemental analysis: found C: 59.22, H: 3.30, N: 3.50 calculated for (C<sub>19</sub>H<sub>11</sub>F<sub>6</sub>NO) C: 59.54, H: 2.89, N: 3.65 (%).

**4.2.3. Synthesis of Zn<sub>3</sub>(BFHQ)<sub>6</sub> (5).** A mixture of Zn(AcO)<sub>2</sub>·2H<sub>2</sub>O (3.7 mg, 0.01 mmol), **4** (3.8 mg, 0.01 mmol), H<sub>2</sub>O (0.5 mL), and MeOH (2 mL) in a capped vial was heated at 80 °C for one day. Red rod-like crystals of **5** were filtered, washed with MeOH and Et<sub>2</sub>O, and dried at room temperature. Yield: 3.0 mg (72%). <sup>1</sup>H NMR (d<sub>6</sub>-DMSO, 300 MHz) δ 6.93 (d, J=7.2 Hz, 1H), 7.04 (d, J=8.7 Hz, 1H), 7.43 (t, J=8.1 Hz, 1H), 8.04 (d, J=16.5 Hz, 1H), 8.10 (s, 1H), 8.19 (d, J=9.0 Hz, 1H), 8.39 (s, 2H), 8.49 (d, J=8.1 Hz, 1H), 8.85 (d, J=16.5 Hz, 1H); <sup>19</sup>F NMR (CDCl<sub>3</sub>, 282 MHz) δ -61.32 (s, 6F); IR (KBr, ν/cm<sup>-1</sup>): 3053, 2917, 1638, 1458, 1308, 1105, 944, 797, 701, 684, 566, 536, 505, 496, 442; elemental analysis: found C: 55.12, H: 2.30, N: 3.50 calculated for (C<sub>38</sub>H<sub>20</sub>F<sub>12</sub>N<sub>2</sub>O<sub>2</sub>Zn) C: 54.99, H: 2.43, N: 3.38 (%).

## 4.3. X-ray crystallography

Red rod-like crystals of Zn<sub>3</sub>L<sub>6</sub>, **5** were obtained in high yield by heating **4** and Zn(AcO)<sub>2</sub>·2H<sub>2</sub>O at 80 °C in H<sub>2</sub>O/MeOH for one day. A single-crystal X-ray diffraction study on **5** revealed a neutral

trinuclear zinc complex with half of a formula unit in the asymmetric unit. The CCDC number is 784898 (Tables 2 and 3).

**Table 2**  
Crystal data and structure refinement for **5**

5 (293 K)	
Empirical formula	C <sub>114</sub> H <sub>60</sub> F <sub>36</sub> N <sub>6</sub> O <sub>6</sub> Zn <sub>3</sub>
<i>M</i>	2489.79
Wavelength (Å)	0.71073
Crystal system	Monoclinic
Space group	C2/C
<i>a</i> /Å	25.641(9)
<i>b</i> /Å	21.243(7)
<i>c</i> /Å	19.411(7)
β/°	101.460(5)
<i>V</i> /Å <sup>3</sup>	10,362(6)
<i>Z</i>	4
ρ <sub>calcd</sub> /g cm <sup>-3</sup>	1.596
μ/mm <sup>-1</sup>	0.814
Reflns collected	21,315
Unique reflns	9120
<i>R</i> <sub>int</sub>	0.0773
<i>S</i>	0.809
<i>R</i> <sub>1</sub> <sup>a</sup> ( <i>I</i> >2σ( <i>I</i> ))	0.0546
<i>wR</i> <sub>2</sub> <sup>b</sup> (all data)	0.1314

<sup>a</sup>  $R_1 = \sum ||F_o| - |F_c|| / \sum |F_o|$ .

<sup>b</sup>  $wR_2 = [\sum w(F_o^2 - F_c^2)^2 / \sum w(F_o^2)^2]^{1/2}$ .

**Table 3**  
Selected bond lengths (Å) and angles (°) for **5**<sup>a</sup>

Zn(1)–O(2)	1.953(4)	Zn(2)–O(1a)	1.992(3)
Zn(1)–O(3)	2.016(3)	Zn(2)–N(1)	2.208(4)
Zn(1)–O(1)	2.041(3)	Zn(2)–N(1a)	2.208(4)
Zn(1)–N(3)	2.147(4)	Zn(2)–O(3)	2.208(3)
Zn(1)–N(2)	2.228(4)	Zn(2)–O(3a)	2.208(3)
Zn(2)–O(1)	1.992(3)		
O(2)–Zn(1)–O(3)	179.15(16)	O(1)–Zn(2)–N(1a)	109.39(14)
O(2)–Zn(1)–O(1)	101.06(15)	O(1a)–Zn(2)–N(1a)	79.35(14)
O(3)–Zn(1)–O(1)	79.14(13)	N(1)–Zn(2)–N(1a)	93.39(19)
O(2)–Zn(1)–N(3)	99.94(16)	O(1)–Zn(2)–O(3)	75.74(13)
O(3)–Zn(1)–N(3)	80.60(15)	O(1a)–Zn(2)–O(3)	95.79(13)
O(1)–Zn(1)–N(3)	122.71(14)	N(1)–Zn(2)–O(3)	154.82(14)
O(2)–Zn(1)–N(2)	80.37(18)	N(1a)–Zn(2)–O(3)	91.45(12)
O(3)–Zn(1)–N(2)	98.79(17)	O(1)–Zn(2)–O(3a)	95.79(13)
O(1)–Zn(1)–N(2)	110.80(14)	O(1a)–Zn(2)–O(3a)	75.74(13)
N(3)–Zn(1)–N(2)	124.99(15)	N(1)–Zn(2)–O(3a)	91.45(12)
O(1)–Zn(2)–O(1a)	167.68(19)	N(1a)–Zn(2)–O(3a)	154.82(14)
O(1)–Zn(2)–N(1)	79.35(14)	O(3)–Zn(2)–O(3a)	94.61(17)
O(1a)–Zn(2)–N(1)	109.39(14)		

<sup>a</sup> Symmetry codes: *a*)  $-x+2, y, -z+1/2$ .

## Acknowledgements

This work was supported by the National Natural Science Foundation of China (20802010, 21032006, 20972178) and 211 project of Guangdong Province.

## Supplementary data

Supplementary data associated with this article can be found in the online version, at doi:10.1016/j.tet.2010.09.039. These data include MOL files and InChIKeys of the most important compounds described in this article.

## References and notes

- Tang, C. W.; VanSlyke, S. A. *Appl. Phys. Lett.* **1987**, *51*, 913.
- Rai, V. K.; Srivastava, R.; Kamalasanan, M. N. *Synth. Met.* **2009**, *159*, 234.
- Matsumoto, N.; Miyazaki, T.; Nishiyama, M.; Adachi, C. *J. Phys. Chem. C* **2009**, *113*, 6261.

4. Liu, Z. W.; Bian, Z. Q.; Hao, F.; Nie, D. B.; Ding, F.; Chen, Z. Q.; Huang, C. H. *Org. Electron.* **2009**, *10*, 247.
5. Tao, Y. T.; Wang, Q.; Shang, Y.; Yang, C. L.; Ao, L.; Qin, J. G.; Ma, D. G.; Shuai, Z. G. *Chem. Commun.* **2009**, 77.
6. Chang, C. H.; Lu, Y. J.; Liu, C. C.; Yeh, Y. H.; Wu, C. J. *Display Technol.* **2007**, *3*, 193.
7. Liedtke, A.; O'Neill, M.; Wertmoller, A.; Kitney, S. P.; Kelly, S. M. *Chem. Mater.* **2008**, *20*, 3579.
8. Gather, M. C.; Alle, R.; Becker, H.; Meerholz, K. *Adv. Mater.* **2007**, *19*, 4460.
9. Mishra, A.; Nayak, P. K.; Periasamy, N. *Tetrahedron Lett.* **2004**, *45*, 6265.
10. Cui, Z.; Kim, S. H. *Chin. Sci. Bull.* **2004**, *49*, 797.
11. Xie, J.; Ning, Z.; Tian, H. *Tetrahedron Lett.* **2005**, *46*, 8559.
12. Radek, P.; Pavel, A. J. *Org. Lett.* **2003**, *5*, 2769.
13. Wang, T. T.; Zeng, G. C.; Zeng, H. P.; Liu, P. Y.; Wang, R. X.; Zhang, Z. J.; Xiong, Y. L. *Tetrahedron* **2009**, *65*, 6325.
14. Zeng, H. P.; Wang, G. R.; Zeng, G. C.; Li, J. *Dyes Pigments* **2009**, *83*, 155.
15. Sakamoto, Y.; Suzuki, T.; Kobayashi, M.; Gao, Y.; Fukai, Y.; Inoue, Y.; Sato, F.; Tokito, S. *J. Am. Chem. Soc.* **2004**, *126*, 8138.
16. Shi, M. M.; Chen, H. Z.; Sun, J. Z.; Ye, J.; Wang, M. *Chem. Commun.* **2003**, 1710.
17. Shi, Y. W.; Shi, M. M.; Huang, J. C.; Chen, H. Z.; Wang, M.; Liu, X. D.; Ma, Y. G.; Xu, H.; Yang, B. *Chem. Commun.* **2006**, 1941.
18. Matsumura, M.; Akai, T. *Jpn. J. Appl. Phys.* **1996**, *35*, 5357.
19. Zhong, C.; Wu, Q.; Guo, R.; Zhang, H. *Opt. Mater.* **2007**, *30*, 870.
20. Ramesh, V.; Umasundari, P.; Das, K. K. *Spectrochim. Acta, Part A* **1998**, *54*, 285.
21. Perkovic, M. W. *Inorg. Chem.* **2000**, *39*, 4962.
22. El-Dissouky, A. *Spectrochim. Acta, Part A* **1987**, *43*, 1177.
23. Wu, Q.; Esteghamatian, M.; Hu, N. X.; Popovic, Z. D. *Chem. Mater.* **2000**, *12*, 79.
24. Huang, Q. L.; Li, J. F.; Marks, T. J. *J. Appl. Phys.* **2007**, *101*, 093101.
25. Sapochak, L. S.; Benincasa, F. E.; Schofield, R. S.; Baker, J. L.; Riccio, K. K. C.; Fogarty, D.; Kohlmann, H.; Ferris, K. F.; Burrows, P. E. *J. Am. Chem. Soc.* **2002**, *124*, 6119.